THE ENGINEER STORY

e-ISSN: 3009 - 0792 Volume 9, 2023, 14-19

ANALYSIS ON GROWTH REGION DISTRIBUTION FOR QUASI-PYROLYSIS SYNTHESIS OF CNT IN METHANE DIFFUSION FLAME

Muhammad Amirrul Amin Moen, Norikhwan Hamzah *
Faculty of Mechanical Engineering, Universiti Teknologi Malaysia, UTM Johor Bahru, Johor, Malaysia, Malaysia.
* Corresponding author: norikhwan@utm.my

ABSTRACT

Flame synthesis provides an economical and scalable method for producing carbon nanotubes (CNTs), yet the inherent challenges of diffusion flames such as highly oxidizing conditions and soot formation pose significant obstacles. This study explores the impact of a novel compartmentalized chamber design on flame-synthesized CNTs, aiming to mitigate these challenges. Positioned above a methane diffusion flame, the stainless-steel chamber isolates CNT growth from the oxidizing environment and reduces soot formation. CNT growth was analyzed on catalyst-coated ceramic beads within the chamber, examining the optimal growth regions at various heights above the burner (HAB) and wire mesh (HAW). Results indicated negligible CNT growth at HAB 0-5 mm due to insufficient temperature and CO formation. Optimal growth over 90% was observed at HAB 10-60 mm, with a peak at HAB 20-30 mm attributed to consistent CO production near the wire mesh. Beyond HAB 60-70 mm, CNT growth decreased due to reduced CO concentration. Additionally, the highest CNT growth corresponded to HAW 0, closest to the mesh where CO concentration was highest, with growth declining as HAW increased (0-20 mm). These findings demonstrate the chamber's effectiveness in creating a CO-rich zone for CNT synthesis, highlighting its potential to optimize flame-based CNT production by isolating growth from adverse flame conditions.

KEYWORD

Flame synthesis, carbon nanotubes, oxidizing flame sheet, synthesis chamber

INTRODUCTION

Carbon nanotubes (CNTs), with their exceptional structural properties, hold significant promise for a wide range of industrial applications, including energy storage, thermal management, and solar technologies. Traditional methods for producing pristine CNTs, such as plasma arc discharge (PAD) and pulsed laser vaporization (PLV), are well-established but often costly and complex [1-5] . For bulk applications requiring lower quality CNTs, chemical vapor deposition (CVD) variations are commonly used due to their precise control over temperature and gas composition crucial for CNT growth. However, CVD processes are limited by slow synthesis rates and high energy consumption due to furnace utilization. As a result, alternative methods that reduce energy consumption are actively being explored. Among these, flame synthesis has emerged as a promising, energy-efficient, and scalable alternative, already applied commercially for producing materials like fumed silica and carbon black [6]. Flame synthesis involves high-temperature combustion, leading to fuel decomposition into carbon atoms and hydrogen molecules, with the carbon atoms attaching to catalyst particles to form CNTs [7]. Despite its potential, achieving optimal CNT morphology in flame synthesis requires precise control over parameters such as the height above the burner (HAB), which influences temperature distribution and reaction kinetics. Previous studies show that controlling HAB can significantly impact CNT morphology by affecting temperature profiles and growth conditions [8-10]. Moreover, the highly oxidizing region of diffusion flames present challenges such as soot formation, which deactivates catalysts and competes with CNT growth [11]. To address these issues, this study investigates a novel compartmentalized chamber design that isolates CNT growth from the flame's oxidizing environment and minimizes soot formation. Positioned above a methane diffusion flame, this

stainless-steel chamber enables a controlled synthesis environment, enhancing CNT growth by creating a CO-rich zone and protecting the catalyst from adverse flame conditions. This research maps the optimal CNT growth regions within the chamber at various HAB and heights above wire mesh (HAW), demonstrating the chamber's effectiveness and potential for advancing flame-based CNT synthesis.

MATERIAL AND METHODOLOGY

The experimental setup for flame-based CNT synthesis is shown in Figure 1. A diffusion flame was generated atop a burner using methane and dry air, according to established protocols. The burner featured two concentric annuli: the outer annulus supplied oxidizer at 3.7 slpm, and the inner annulus provided pure methane gas (99.5% purity) at 0.4 slpm. A novel synthesis chamber, a cylindrical stainless-steel tube (1.2 mm wall thickness, 9.5 mm outer diameter, and 140 mm length), was aligned above the burner at a set distance. A stainless-steel wire mesh with 0.9 mm openings (#20 mesh) at the chamber inlet faced the burner outlet, preventing flame formation within the chamber, redistributing the flame flow, and creating an engulfing flame sheet around the chamber for optimal CNT growth temperatures. The absence of a flame sheet inside the chamber allowed prolonged CNT growth by eliminating highly oxidizing conditions and minimizing soot formation, which deactivate catalyst nanoparticles. The CNT growth temperature was measured using a K-type thermocouple on the chamber's central axis. Nickel nitrate-coated SiO_2 ceramic beads (3 mm diameter) served as substrate-supported catalysts, comprising 80% SiO_2 and 20% Al_2O_3. The beads were sonicated in ethanol for 10 minutes to clean them, then impregnated with a 10 wt% nickel nitrate solution, stirred for 12 hours, dried at 100°C for 1 hour, and reduced with nitrogen gas at 500°C for 30 minutes. HAB was measured as the distance from the burner outlet to the synthesis chamber inlet, with the chamber placed 10-70 mm above the burner. HAW analysis varied the placement of catalyst-coated beads within the chamber, measured from the chamber inlet to the outlet in 10 mm increments.

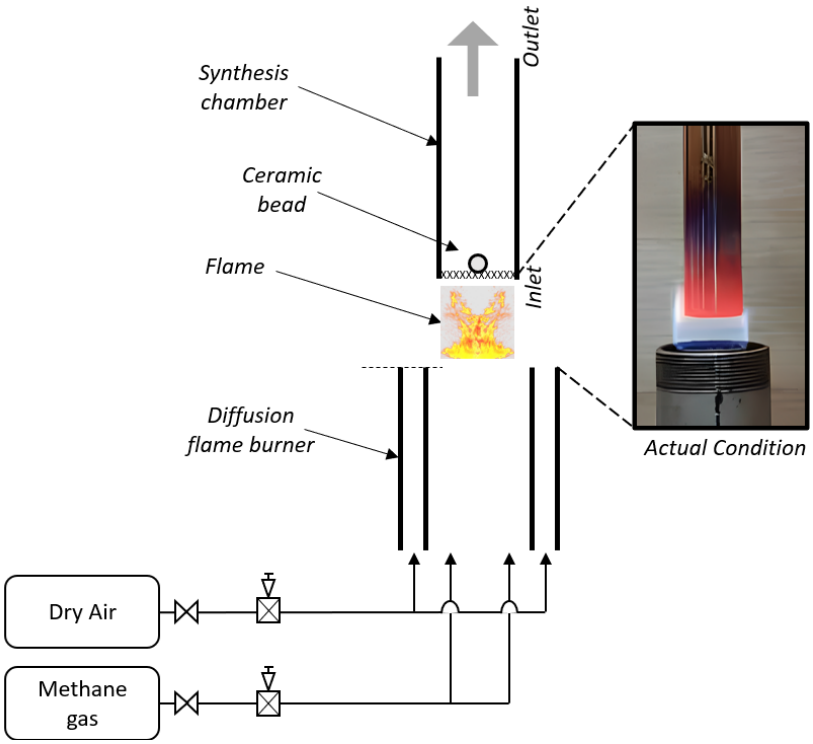

Figure 1: Experimental Setup.

Each experiment used one bead for consistent growth distribution, analyzed via FESEM, HRTEM, and Raman spectroscopy. Macro-image analysis, using a DSLR camera (Canon EOS 600D) with macro lenses, assessed CNT growth regions, characterized by dark-black surfaces on the beads. Images were converted to 8-bit using ImageJ software with a threshold value of 60, determined through SEM analysis, to accurately measure CNT coverage. This simplified method minimized sample preparation and repetitive SEM analysis. The exhaust gas composition was analyzed using an EMS 520 Exhaust Gas Analyzer, with steel suction tubes positioned at HAW 0-20 mm across HAB 0-70 mm, ensuring measurement accuracy through triplicate measurements.

RESULT AND DISCUSSION

The experimental analysis of CNT growth in relation to Height Above Burner (HAB) and Height Above Wire (HAW) revealed key trends in Figure 2. At HAB 0-5 mm, no CNT growth was observed, attributed to insufficient temperature and CO formation. However, between HAB 10-60 mm, consistent CNT growth exceeding 90% was achieved, peaking around HAB 20-30 mm, likely due to the steady CO production facilitated by the wire mesh. Beyond HAB 60 mm, a gradual decline in CNT growth was noted, corresponding with a reduction in CO concentration. The impact of HAW on CNT growth was found to be dependent on HAB. At HAW 0, closest to the wire mesh, the highest CNT growth was recorded for each HAB, correlating with the peak CO concentrations. Conversely, as HAW increased from 0 to 20 mm, there was a notable decline in CNT growth, mirroring the drop in CO concentration with increasing HAW. This trend underscores the critical role of both CO concentration and temperature distribution in optimizing CNT growth within the synthesis chamber.

The study of CNT growth at various heights above the burner (HAB) and heights above the wire (HAW) reveals significant thermal variations impacting the synthesis process as shown in Figure 3. At HAB 0 mm, the temperature is the lowest due to incomplete methane combustion; methane is drawn into the synthesis chamber rather than burning in the flame, resulting in less heat release. At HAB 50 mm, the temperature is at its peak, 41% higher than at HAB 0 mm, because more complete methane combustion occurs, releasing more energy and raising the temperature. However, at HAB 60-70 mm, the temperature declines as the hot flame sheet forms significantly below the synthesis chamber. Regarding HAW, from HAB 0-20 mm, the temperature rises with increasing HAW, reflecting the progression of methane combustion and the formation of a flame sheet around the synthesis chamber. In contrast, at HAB 40-70 mm, the temperature decreases with increasing HAW due to the formation of the hot flame sheet primarily under the tube. At HAB 60 mm and above, the flame sheet fully forms below the synthesis chamber, further reducing the temperature within the chamber. This nuanced temperature distribution, influenced by both HAB and HAW, underscores the importance of precise positioning to optimize the CNT synthesis environment.

The relationship between CO formation and the height above the burner (HAB) reveals critical insights into the combustion process and its efficiency in CNT synthesis as shown in Figure 4. At HAB 0 mm, which is closest to the burner, CO formation is negligible due to low temperatures and incomplete combustion; methane enters the chamber but does not combust effectively due to insufficient heat. As the HAB increases from 0 to 40 mm, CO formation progressively rises, correlating with the increasing temperature that supports more complete combustion and, consequently, greater CO production. However, at HAB 50-70 mm, CO formation diminishes. This decline is attributed to the formation of a hot flame sheet beneath the synthesis chamber, indicating complete combustion beneath the wire mesh. This complete combustion results in minimal CO formation within the chamber. Thus, the CO production is closely tied to the height above the burner, with optimal CO levels achieved at intermediate heights where temperature and combustion conditions are most favorable.

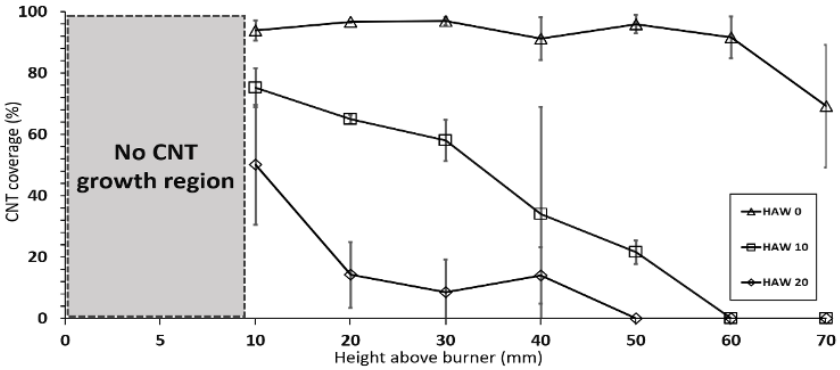

Figure 2: CNT growth region at HAB 0 to 70mm for specific HAW 0 to 20. No CNT growth at under HAB 10mm

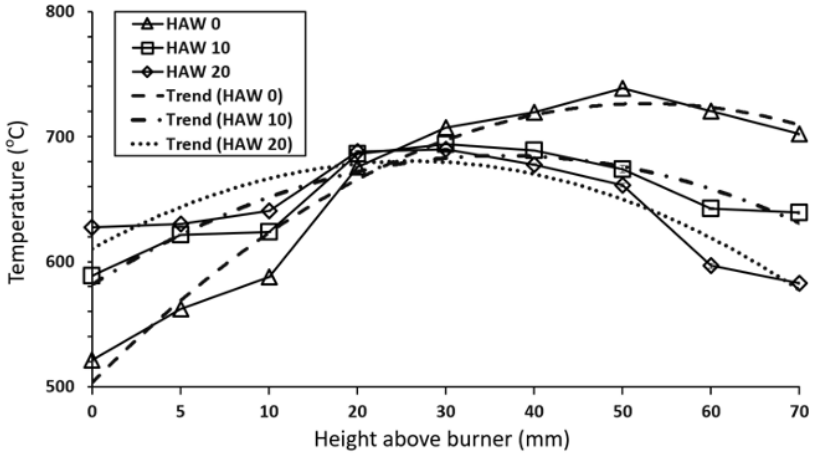

Figure 3: The temperature measurement at central axis of synthesis chamber at HAB 0 to 70mm for HAW 0 to 20mm

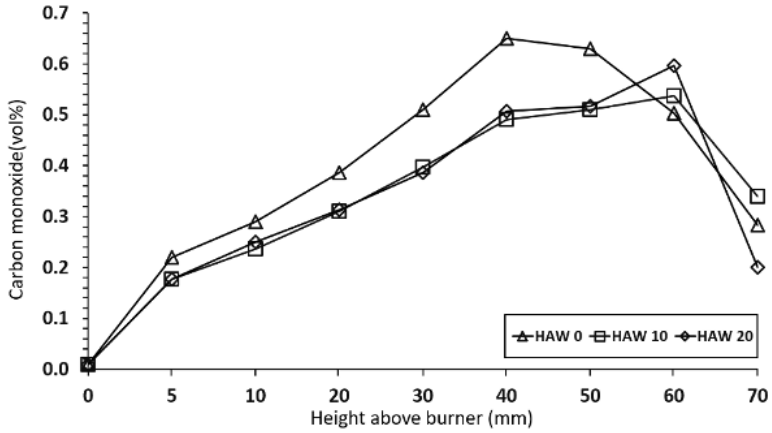

Figure 4: Carbon Monoxide measurement inside the synthesis chamber at HAB 0 to 70mm for HAW 0 to 20mm

CONCLUSION

The study confirms the chamber's effectiveness in optimizing CNT synthesis. Notably, consistent and optimal CNT growth (>90%) was achieved at a Height Above Burner (HAB) of 10-60 mm, peaking at 20-30 mm. This range aligns with the highest carbon monoxide (CO) concentration, a key precursor for CNT growth, facilitated by steady CO formation at the wire mesh. The impact of Height Above Wire Mesh (HAW) was also significant within this optimal HAB range. Maximum CNT growth occurred at HAW 0 (closest to the mesh), where CO concentration was highest, but growth declined with increasing HAW (0-20 mm) due to reduced CO levels. The chamber successfully protected the CNT growth zone from adverse factors such as soot formation and excessive oxidation, evidenced by the lack of CNT growth at HAB 0-5 mm, likely due to low temperature and incomplete methane combustion at this close proximity to the burner. Temperature distribution in the chamber rose with increasing HAB, reflecting more complete combustion, but decreased with increasing HAW, corresponding to the hot flame sheet forming below the chamber. CO formation followed a similar trend, increasing with HAB due to enhanced combustion efficiency at greater distances from the burner, and decreasing with HAW due to the complete formation of the flame sheet below the wire mesh, indicating reduced CO production.

ACKNOWLEDGEMENT

The authors would like to express their gratitude to the Automotive Development Centre (ADC), Universiti Teknologi Malaysia and University Industry Research Laboratory for their support on equipment. The highest appreciation goes to Universiti Teknologi Malaysia for the financial support through a KPT Fundamental Research Grant.

REFERENCE

[1] A. Venkataraman, E. V. Amadi, Y. Chen, and C. Papadopoulos, "Carbon Nanotube Assembly and Integration for Applications," Nanoscale Res Lett, vol. 14, no. 1, 2019, doi: 10.1186/s11671-019-3046-3.

[2] S. Kumar, M. Nehra, D. Kedia, N. Dilbaghi, K. Tankeshwar, and K. H. Kim, "Carbon nanotubes: A potential material for energy conversion and storage," Prog Energy Combust Sci, vol. 64, pp. 219–253, 2018, doi: 10.1016/j.pecs.2017.10.005.

[3] M. Pant, R. Singh, P. Negi, K. Tiwari, and Y. Singh, "A comprehensive review on carbon nano-tube synthesis using chemical vapor deposition," Mater Today Proc, vol. 46, no. xxxx, pp. 11250–11253, 2021, doi: 10.1016/j.matpr.2021.02.646.

[4] S. Yousef and A. Mohamed, "Mass production of CNTs using CVD multi-quartz tubes," Journal of Mechanical Science and Technology, vol. 30, no. 11, pp. 5135–5141, 2016, doi: 10.1007/s12206-016-1031-7.

[5] O. O. Cilsal, M. C. Cakir, and A. Uguz, "Innovative low-cost, cold-walled CVD process development and CNT production by ethanol decomposition on iron-nanoparticles," Surface Engineering, vol. 38, no. 5, pp. 472–481, 2022, doi: 10.1080/02670844.2022.2113755.

[6] D. Chauhan, A. Pujari, G. Zhang, K. Dasgupta, V. N. Shanov, and M. J. Schulz, "Effect of a Metallocene Catalyst Mixture on CNT Yield Using the FC-CVD Process," Catalysts, vol. 12, no. 3, pp. 1–20, 2022, doi: 10.3390/catal12030287.

[7] M. H. Ibrahim, N. Hamzah, M. Z. M. Yusop, N. L. W. Septiani, and M. F. M. Yasin, "Control of morphology and crystallinity of CNTs in flame synthesis with one-dimensional reaction zone," Beilstein Journal of Nanotechnology, vol. 14, pp. 741–750, 2023, doi: 10.3762/BJNANO.14.61.

[8] S. Okada et al., "Flame-assisted chemical vapor deposition for continuous gas-phase synthesis of 1-nm-diameter single-wall carbon nanotubes," Carbon N Y, vol. 138, pp. 1–7, 2018, doi: 10.1016/j.carbon.2018.05.060.

[9] N. Hamzah et al., "Effect of fuel and oxygen concentration toward catalyst encapsulation in water-assisted flame synthesis of carbon nanotubes," Combust Flame, vol. 220, pp. 272–287, 2020, doi: 10.1016/j.combustflame.2020.07.007.

[10] H. G. S. and R. A. D. R. J. Santoro, “Soot Particle Measurements in Diffusion Flames,” Combust Flame, vol. 51, pp. 203–218, 1983.
[11] B. B. Chakraborty and R. Long, “The formation of soot and polycyclic aromatic hydrocarbons in diffusion flames- part one,” Combust Flame, vol. 12, no. 3, pp. 226–236, 1968, doi: 10.1016/0010-2180(68)90019-9.